Article no. 25

THE CIVIL ENGINEERING JOURNAL 3-2019

EXPERIMENTAL STUDY ON SEISMIC BEHAVIOR OF JOINT BEAM WITH JOINT SHEAR WALL STRUCTURE

JIA Ru-da

Zhejiang Industry Polytechnic College,Shaoxing Zhejiang ,312069,China;
jiarudazjgyzyxy@163.com

ABSTRACT

The reinforced concrete connecting beams that exhibit a larger shear span ratio (μ≥2.5) are easy to dissipate energy under seismic action, thereby protecting other components. However, the connecting girder will be seriously damaged under this action, which hinders the rapid recovery of the building function after the earthquake. By installing shear damper in the span of the connecting beam, the deformation and damage of the connecting beam can be concentrated in the damper. To test the seismic performance of the scheme, three specimens with a shear span ratio of 3.0 were designed in the present study, namely 2 ordinary RC beams and 1 energy dissipation beam with damper. According to the comparison of the performance in the three components in the quasi-static test, the energy dissipation connecting beams with reasonable design can effectively reduce the damage degree of concrete beam sections and wall limbs. In the meantime, the bearing capacity problem of RC beams was not found in energy dissipation connecting beams, which helps to achieve the ideal structural damage control.

KEYWORDS

Energy-dissipating coupling beam, Large aspect ratio, Metallic shear link, Damage control

INTRODUCTION

The joint shear wall is a common anti-lateral force member of high-rise structures, of which the ideal failure mode refers to the ductile failure mode of the successive yield of the connecting beam and the plastic hinge at the bottom of the wall limb [1]. The failure of reinforced concrete connecting beams that exhibit a high shear span ratio is manifested as bending failure control, which shows excellent ductility performance [2], and is capable of dissipating more seismic energy input and regulating the damage degree of wall limbs [3]. However, its own serious damage and bearing capacity problems limit the reliability of its seismic performance. To solve the mentioned problems, Pan Chao [4] and Ji Xiaodong [5] all used the setting of energy dissipation damper in the middle position of the connecting beam span. The former using theoretical derivation and numerical simulation, analysed the effect of damper stiffness on the performance of the wall with energy dissipation joint, whereas no attention was paid to the damage of the concrete part and the wall limb. To reduce the damage of concrete connecting beam, the latter completely adopted steel connecting beam construction.

Thus, 3 scale of 1/2 test specimens were designed and produced here for large shear span RC beams with energy dissipation components in span, and the shear span ratio was set as 3.0. Two ordinary RC connecting beams, namely CB3.0 and CB3.0S, served as floor and floor connecting beams, respectively, and energy dissipating connecting beams, DCB3.0S, acted as RC connecting beams with shear metal damper in span. The ability of energy dissipation connecting beam in concrete damage control and bearing capacity was tested by comparing the mechanical property and damage degree in each specimen under low cycle reciprocating load.

BEARING CAPACITY DESIGN

Coupling beam energy dissipation

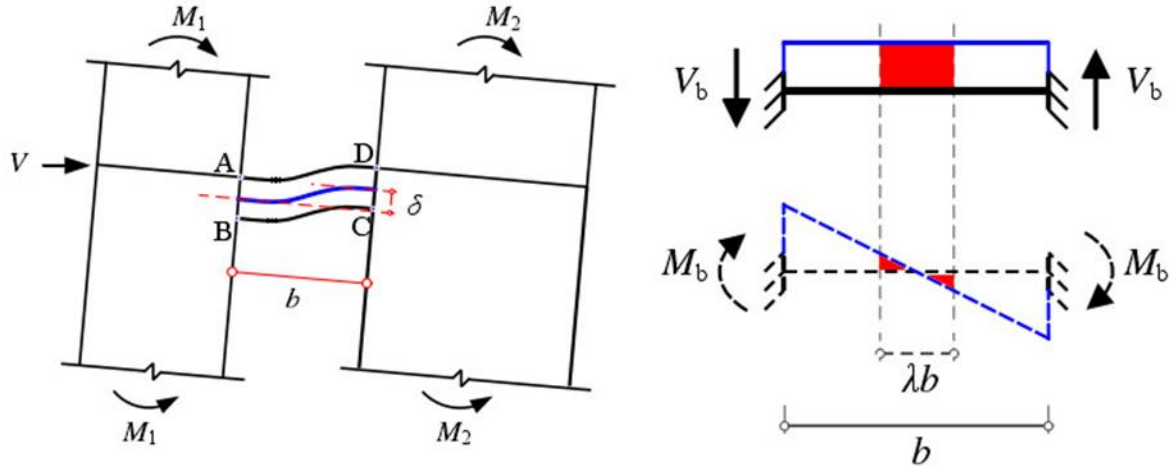

(a) Transformation (b) Shear and moment

Fig.1 - The deformation and internal force of the connecting beam under horizontal load

Regardless of the axial deformation and corresponding axial force of the connecting beam, the connecting beam would be deformed (Figure 1a) and bear the bending moment and shear action (Figure 1b) under the horizontal load. By analysing the internal force distribution of the connecting beam and its effect on the stiffness of the connecting beam, it is obvious that the shear damper was installed in a certain area in the middle of the connecting beam (tentatively defined as λb in length, b in span of the connecting beam), which minimizes the damage to the stiffness of the connecting beam and the bending shear coupled on the damper.

RC coupling beam design

The shear design value of the end section of the connecting beam is calculated according to Equation (1) stipulated in China's Code for design of concrete structures GB 50010-2010.

$$V = \eta_{vb} \frac{M_b^l + M_b^r}{l_n} + V_{Gb} \tag{1}$$

Where, $M_{lb}$and M_{rb} denote the bending moment design values of the left and right side sections of the connecting beam, respectively . V_{Gb} is the design value of shearing force of beam end calculated according to simple beam under the action of representative value of gravity load; l_n denotes the net span of the connecting beam; η_{vb} is the increase coefficient of connecting beam. For the shear span of a relatively large connecting beam, its yield bearing capacity is primarily controlled by the normal section and bending performance.

Accordingly, Equation (1) can be used to estimate the yield bearing capacity of the RC connecting beam test piece here, and the effect of gravity load was not considered here.

$$V_{u,c} \le 0.7 f_t b h_0 + f_{yv} \frac{A_{sv}}{s} h_0 \tag{2}$$

An energy dissipation beam with a damper design

$$V_y \le V_{cb} \tag{3}$$

$$\Omega \cdot V_y \leq V_{u,c} \tag{4}$$

When designing an energy dissipation connecting beam with a damper, the yield bearing capacity of the damper V_y, should be lower than the designed flexural bearing capacity of the normal section of the RC connecting beam V_{cb} (which satisfies Equation (3)) to ensure that the damper enters the yield state before the concrete part. In the meantime, to reduce the damage to concrete section and to ensure that the beam final failure is not attributed to shear failure of concrete segment, the ultimate bearing capacity of the damper $\Omega \cdot V_y$, should not be higher than that of shear bearing capacity of concrete section $V_{u,c}$ (content type (4)).

Experimental Methods

Specimen size and reinforcement

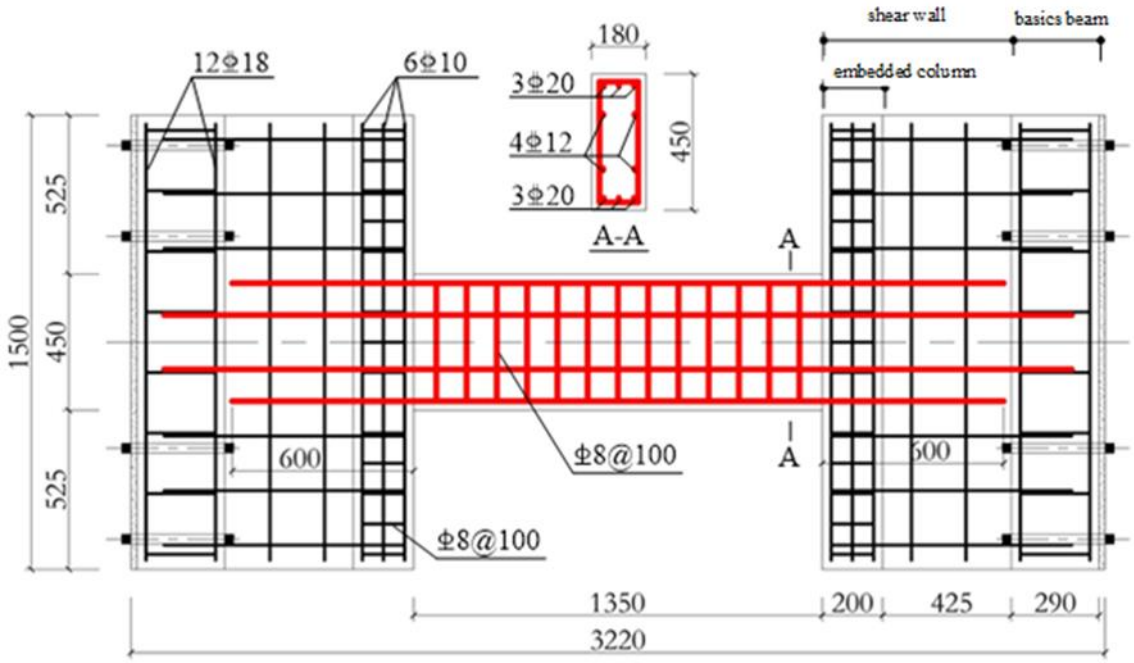

(a)Test body CB3.0

Fig.2 – Configuration and reinforcements of coupling beam specimens

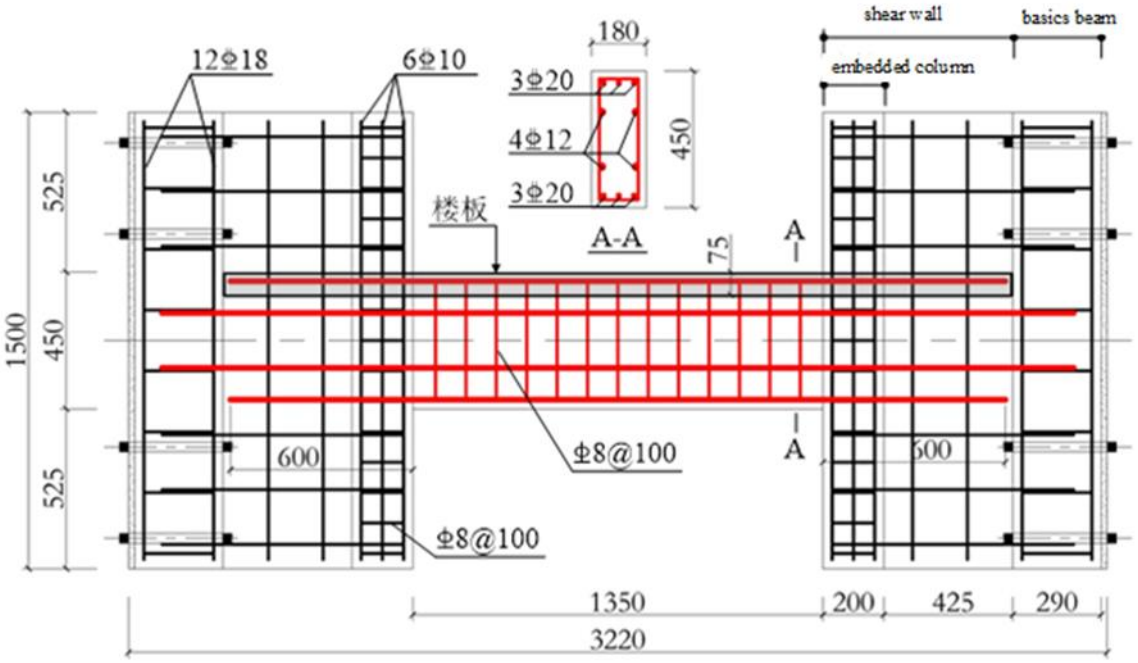

(b)Test body CB3.0S

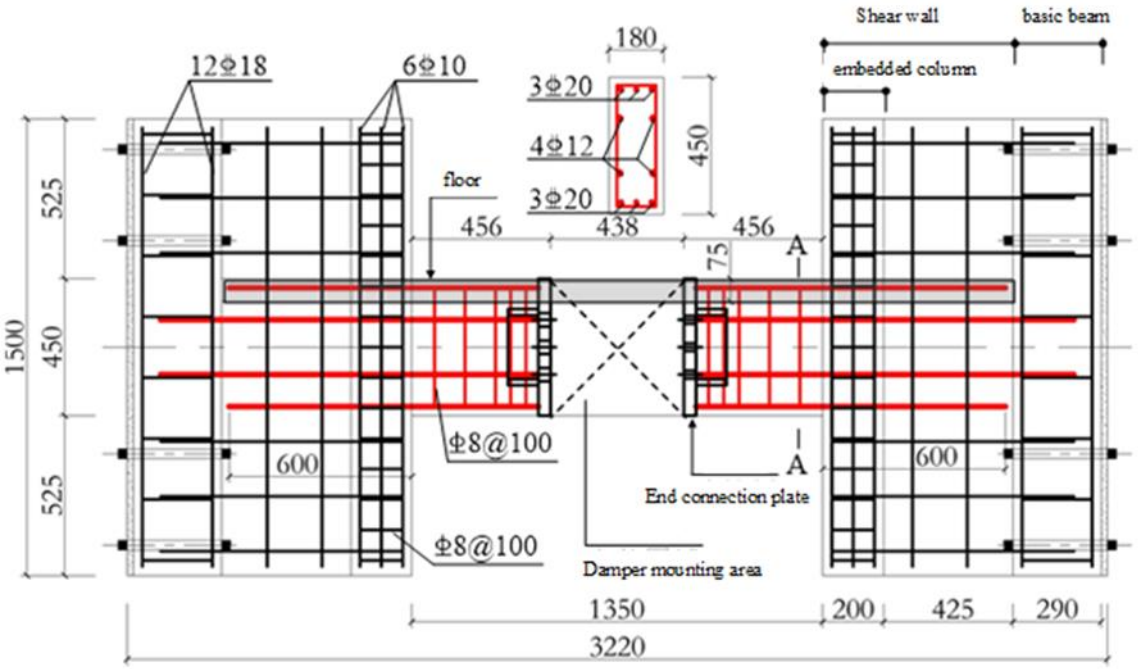

(c)Test body DCB3.0S

Fig.2 – Configuration and reinforcements of coupling beam specimens

Three connecting beam test bodies were designed, named as CB3.0, CB3.0S and DCB3.0S, respectively, abiding by China's Code for design of concrete structures GB 50010-2010. CB and DCB represent ordinary RC connecting beams and RC connecting beams with damper,

respectively. The net span of the connecting beam is 1350mm, and the section height h and width b are 450mm and 180mm, respectively.

The main size and reinforcement information of the three test bodies are shown in Figure 2. These test bodies consist of connecting beam, two side connecting wall limbs and foundation beam. The reinforcement ratio of horizontal and vertical distributed reinforcement of the shear wall section was set as 0.3%, and the dark column with 200mm width was placed near the connecting beam. The reinforcement ratio of the longitudinal reinforcement was set as 1.2%, and the volume hoop ratio as 1.6%. Common stirrup B8@100 was set in the connecting beam part, and the length of the anchor leg part of the longitudinal reinforcement was no less than 600mm. Floor plates were set in the test bodies CB3.0S and DCB3.0S, 75mm in thickness of and 1380mm in width. The floor slab reinforcement should not be overly close after considering the scale reduction. Double-layer bi-directional layout of floor reinforcement is B6@220mm. Given that the deformation of the test body DCB3.0S is concentrated in the position of the mid-span damper, had a 1350mm x 380mm hole was opened on the floor slab within the range of the connecting beam to avoid premature cracking and punching and cutting failure of the floor slab in this area. The main properties of materials used in the test body are listed in Table 1.

Tab. 1- Measured strength of steel and concrete

materials	Diameter	Yield strength(Mpa)	Ultimate strength(Mpa)	Remark
Rebar	6mm	436	620	Slab reinforcement
	8mm	485	785	Stirrup/wall limb distribution reinforcement
	10mm	470	727	Embedded column longitudinal reinforcement
	18mm	496	675	Diagonal reinforcement
	20mm	482	620	Even the beam longitudinal reinforcement
Steel plate Q235-B	Thickness	Yield strength(Mpa)	Ultimate strength(Mpa)	Elasticity modulus
	16mm	355	507	$2.16\times10_5N/mm_2$
Concrete C40	Specimen number	Test value against pressure	Axial compressive strength	Axial compressive strength
	CB3.0	46.67	31.21	2.88
	CB3.0S DCB3.0S	50.02	33.45	2.99

LOADING AND MEASUREMENT PROGRAM

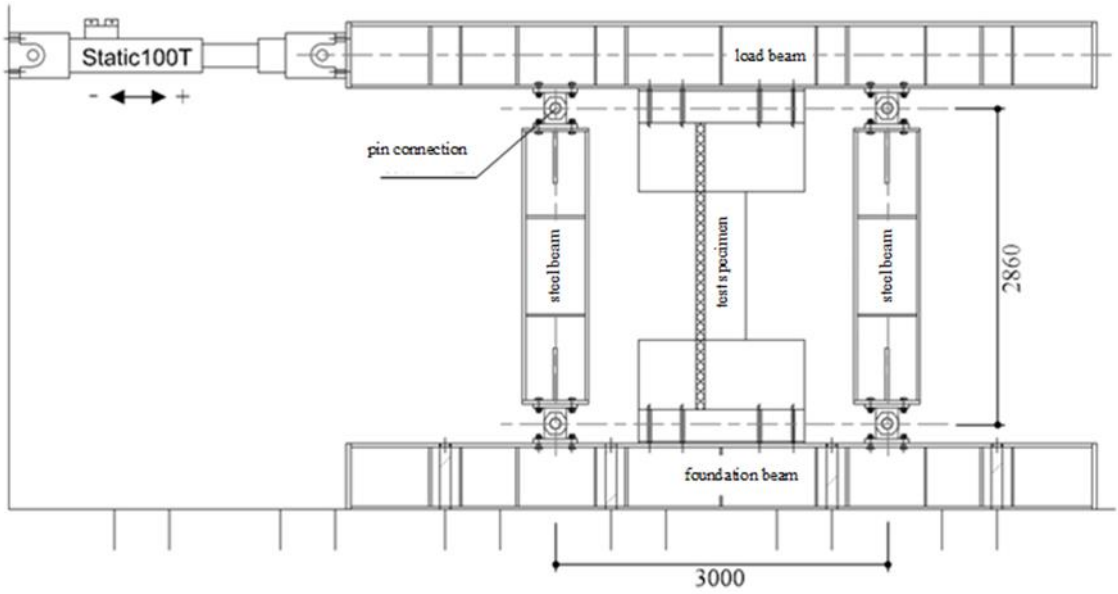

Fig.3 –Test setup

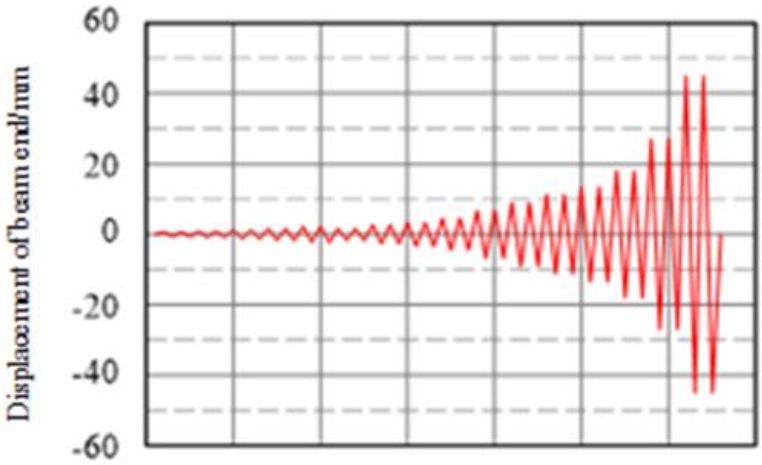

Fig. 4 – Loading scheme

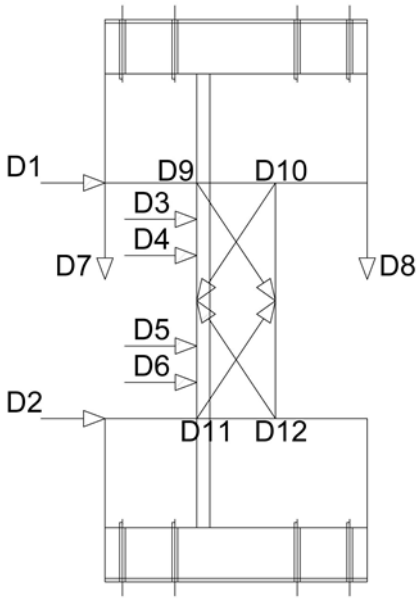

(a) CB3.0(/S)Displacement measurement program

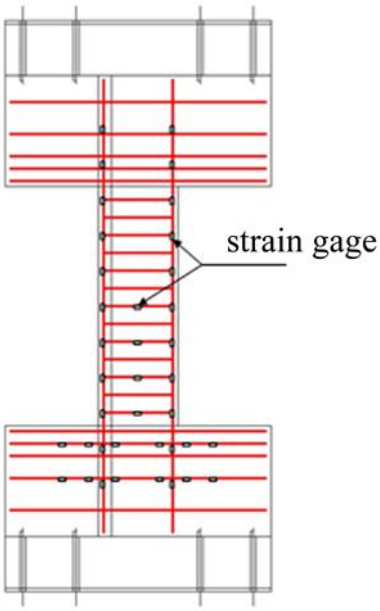

(b) CB3.0(/S) Strain measurement program

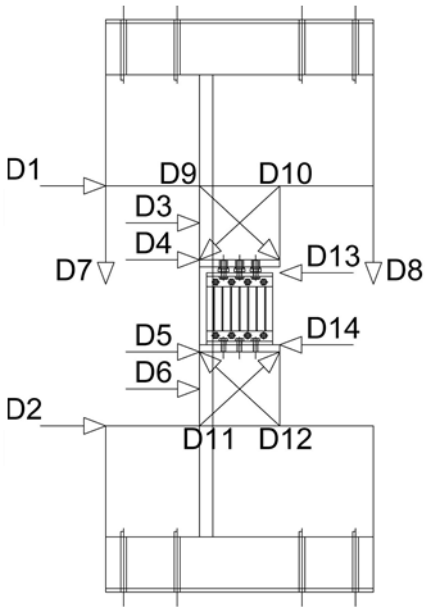

(c) DCB3.0S Displacement measurement program program

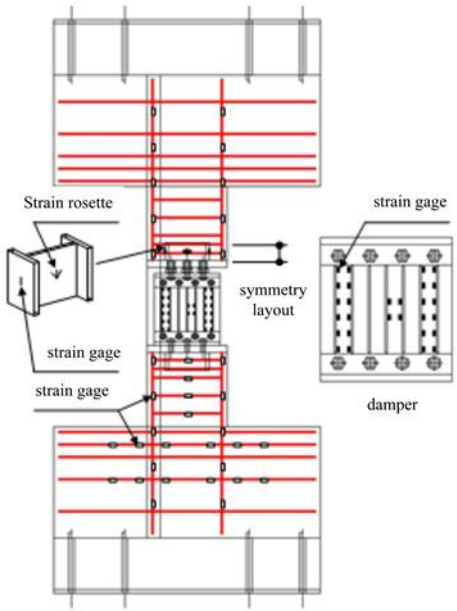

(d) DCB3.0S Strain measurement program

Fig.5 –Measurement

Since Lequesne [5] measured the axial force and deformation of the coupling beam in its multi-layer double-limb wall test, the boundary condition was applied by the parallelogram mechanism loading frame as shown in Figure 3, and the loading history is shown in Figure 4. Each cycle of the cycle was loaded twice, and the strain and displacement measurement scheme is shown in Figure 5.

TEST PHENOMENON

（a）1/800　（b）1/200　（c）1/120　（d）1/50

Fig.6 – Crack development of specimen CB3.0

The fracture development of the CB3.0 connecting beam and wall limb is shown in Figure 6. When the displacement Angle θ of the connecting beam reaches 1/800, several horizontal bending cracks will appear at the end of the connecting beam, and part has been through the section. When the displacement Angle θ of the connecting beam reaches 1/200, cross-inclined cracks will be formed at both ends of the connecting beam. When the displacement Angle θ of the connecting beam reaches 1/120, the longitudinal bar of the connecting beam will enter the yield state. The number of inclined cracks increased but did not diffuse to the mid-span position. Cracks in the wall limb area did not develop significantly. When the displacement Angle θ of the connecting beam reaches 1/50, the number of oblique cracks in the middle of the connecting beam will be up-regulated rapidly, and the connecting beam will be divided into many diamond blocks. When the first circle of the displacement Angle is negatively loaded, the specimen will show obvious transfixion fracture, and the whole specimen will be damaged by shear.

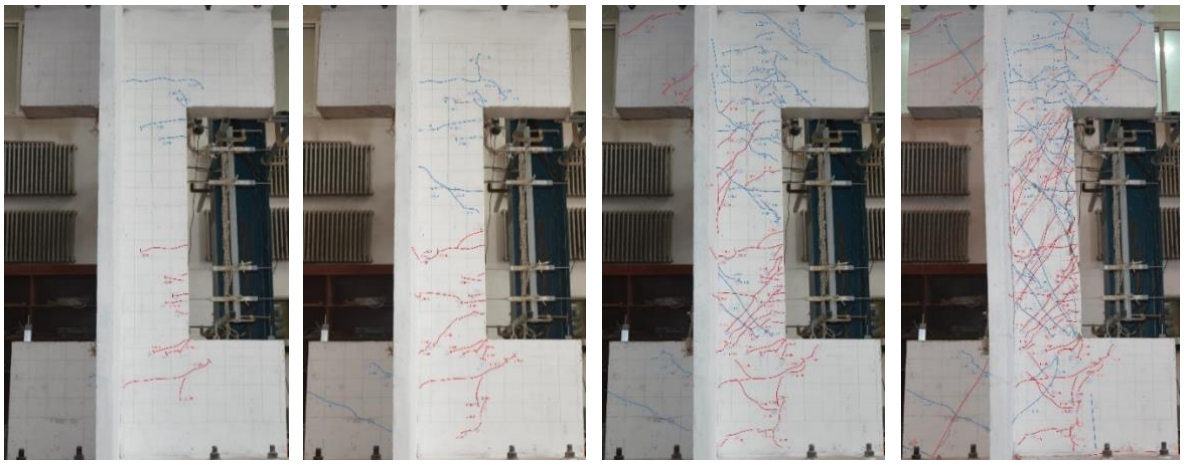

（a）1/800　（b）1/300　（c）1/100　（d）1/30

Fig.7 –Crack development of specimen CB3.0S

The crack development of CB3.0s connecting beam and wall part is shown in Figure7. When the displacement Angle θ of the connecting beam reaches 1/800, along the direction of the connecting beam span, the horizontal curved crack will develop gradually from the upper/lower

beam end to the middle span, and the crack at the end of the connecting beam will extend to the shear wall. When the displacement Angle θ of the connecting beam reaches 1/300, multi-channel horizontal cracks will extend to the full height of the perforating connecting beam. Inclined cracks will appear and widen at the end of the span and middle beam with the increase in working condition. When the displacement Angle θ of the connecting beam reaches 1/100, the longitudinal bar of the connecting beam will enter the yield state. The positive and negative syncline cracks of the connecting beam were increased and intersected, respectively, thereby gradually covering the entire surface of the connecting beam. The oblique cracks within the range of the wall limb also spread to the interface between the wall limb and the loading bottom beam, where the corner crack of the connecting beam was finally 0.75-1.0mm, and the wall limb crack was 0.45mm. When the displacement Angle θ of the connecting beam reaches 1/30, the inclined crack on the north side span of the connecting beam will increase to be the main crack, and the longitudinal split will appear along the span direction at the edge of the connecting beam.

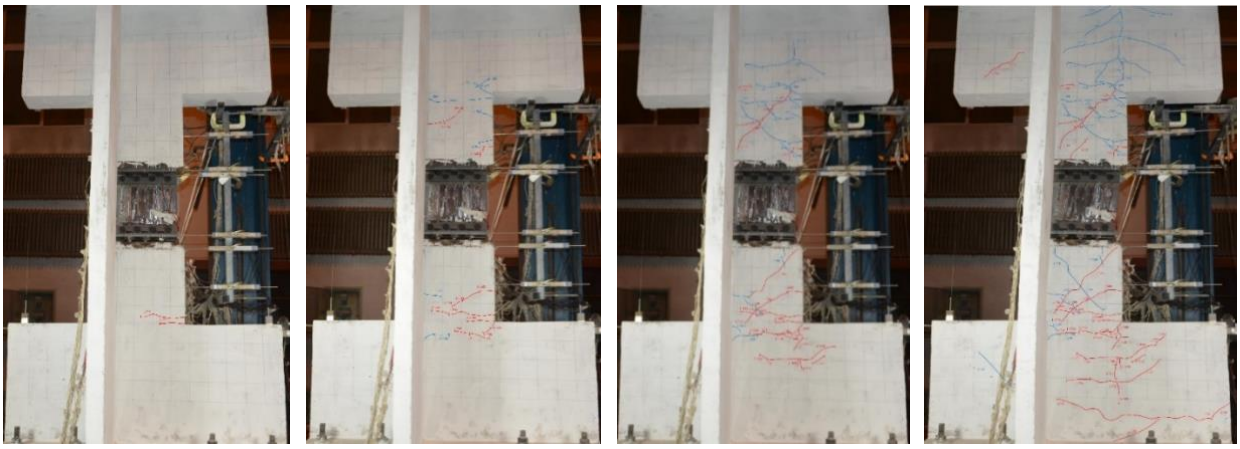

（a）1/800　（b）1/200　（c）1/120　（d）1/30

Fig.8 –Crack development of specimen DCB3.0S

The crack development of the specimen DCB3.0S connecting beam and wall limb is shown in Figure 8. When the displacement Angle θ of the connecting beam reaches 1/800, the beam end of the concrete under the connecting beam will have a positive horizontal crack across the axis of the specimen. When the displacement Angle θ of the connecting beam reaches 1/200, the longitudinal bar of the connecting beam will be yielded. Horizontal seam was formed at both ends of the concrete interface of the connecting beam, and its width was up to 0.25-0.35mm. The slant crack in the connecting beam concrete section is 0.15~0.2mm in width. When the displacement Angle θ of the connecting beam reaches 1/120, inclined cracks will appear at both ends of the connecting beam, and the cracks in the upper concrete section will develop more significantly than those in the lower concrete section. The horizontal curved crack at the end of the link diffuses to the wall limb, and the width of the crack in the corner increases to 0.4mm. When the displacement Angle θ of the connecting beam reaches 1/30, the concrete sections on both sides of the connecting beam will form cross-inclined cracks. In the meantime, the cracks at the end of the beam significantly diffuse to the part of the wall limb, thereby forming a radial shape. The crack width of the corner of the connecting beam is 0.7~1.0mm, the diagonal crack width is 0.65~0.75mm, and the maximum crack width of the wall part is 0.45mm. Finally, the bearing capacity of the damper fractured specimen will decrease to zero.

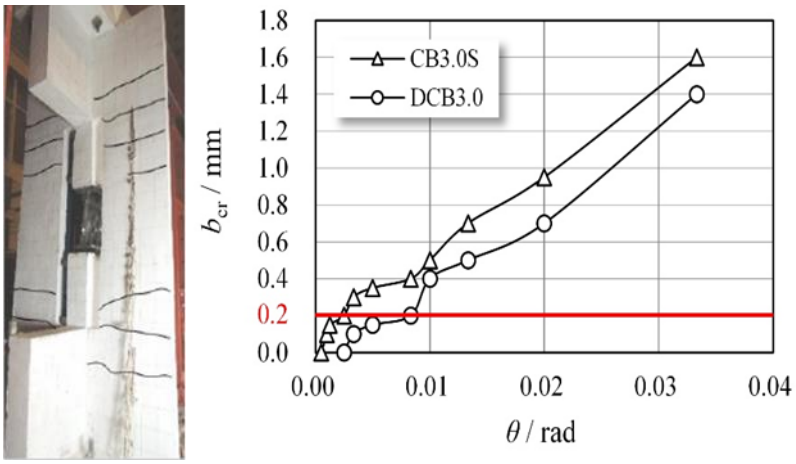

Fig. 9 – Final shape of cracks in DCB3.0S floor and comparison of crack width of floor specimens

Figure 9 shows the floor crack width of two floor specimens (CB3.0s and DCB3.0s) here under different connecting beam displacement Angle θ. The selected crack width is the maximum crack width measured on the upper surface of the floor. According to China's code for concrete structure design (GB50010-2010)[7], the maximum crack width in the limit state of normal use is 0.2mm, and the maximum crack width of the test piece CB3.0s reaches 1/400rad at the Angle θ, while the floor slab of the test piece DCB3.0s has just shown visible cracks (0.03mm). When the test piece DCB3.0s enters the yield state (1/120rad), the crack width of the floor slab will be 0.2mm.

ASEISMIC ANALYSIS

Force-displacement relation

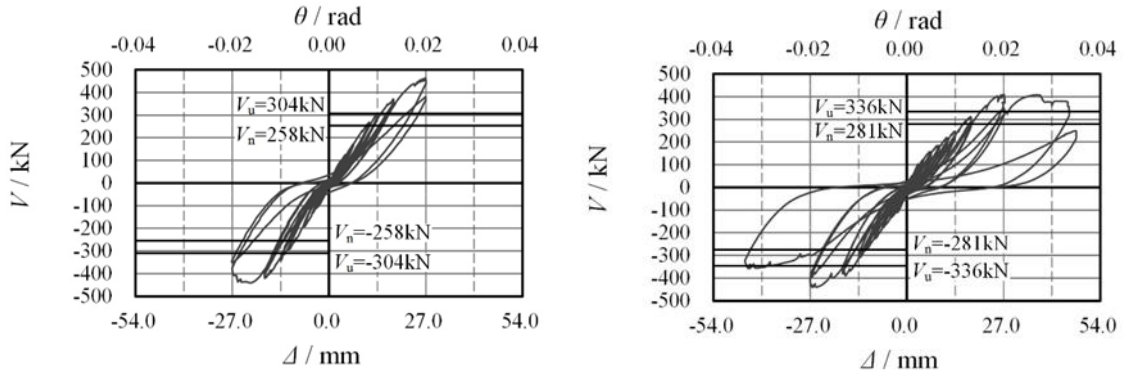

(a) CB3.0 Force-displacement relation *(b) CB3.0S Force-displacement relation*

Fig.10 – Hysteretic loops and skeleton curves of specimens

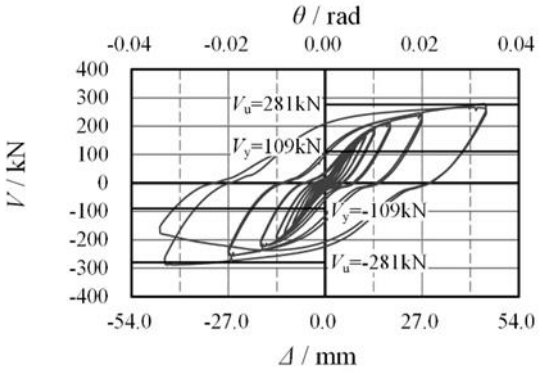

(c) DCB3.0S Force-displacement relation

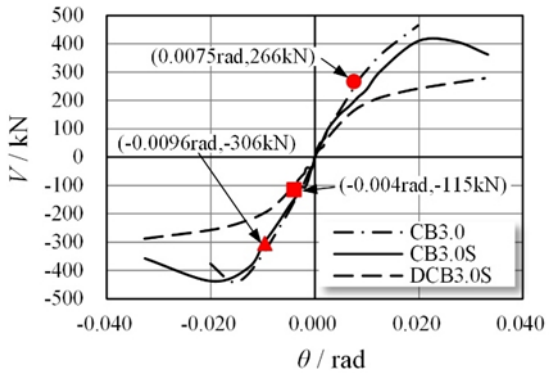

(d) Skeleton curve correlation

Fig.10 – Hysteretic loops and skeleton curves of specimens

Shear Angle hysteresis curve of the specimens is shown in Figures 10 (a) ~ (c), as shown in the shear V test load of horizontal load, coupling beam displacement Δ as calculated on the end of the displacement difference, even the beam displacement Angle θ is through displacement Δ divided by net cross coupling beam ln calculated. The reinforcement ratio and hoop ratio of the test design meet the standard requirements, but the hysteresis curve of RC specimens (CB3.0 and CB3.0S) is obviously pinched. Before the failure of the specimen, the shearing force of the specimen increases obviously with the increase in the Angle of the beam. After the crack of the specimen reaches shear failure to a certain extent, the bearing capacity decreases. Due to the participation of concrete section, the shearing force - displacement angle curve of the specimen DCB3.0S also has a certain degree of pinching, whereas the hysteresis curve is relatively full on the whole, with good deformation capacity and energy dissipation capacity. Comparing the yield point of specimens CB3.0 and CB3.0S in Figure 10 (d) (the displacement Angle and load of the longitudinal bar of the connecting beam at the first yield of the longitudinal bar measured by the test), it is found that the floor slab can raise the yield load of the connecting beam and increase its yield displacement Angle, whereas it does not increase the initial stiffness of the connecting beam and the peak load. Both CB3.0 and CB3.0S were shear failure, and the peak load was determined by its shear capacity. Accordingly, the floor slab made no significant contribution. The floor slab has no effect on the stiffness of the specimen is because the floor slab width is larger than the concrete loading beams on both sides of the specimen, and the load cannot be transferred in these free areas. Thus, the effective width of the floor slab is far less than its actual width.

In Figures 10 (a) ~ (c), V_n, V_u and V_y represent the nominal yield shear of the connecting beam (the corresponding shear value when the specimen reaches the calculation of yield bending moment M_n), shear bearing capacity and the yield bearing capacity of the damper, respectively. The three kinds of bearing capacity are respectively calculated by Response2000 section calculation software [8], GB50010-2010 equation of code to design concrete structures and the design equation of yield bearing capacity of steel plate damping wall suggested by Hitaka [9]. According to the comparison of the above design values with the measured loads shown in Figure9, the yield bearing capacity of RC beam can be accurately designed, while the peak load is significantly higher than the designed bearing capacity, suggesting that the super-strong phenomenon of RC beam after it enters plasticity is significant. The yield and peak bearing capacity of the connecting beam with damper can be estimated accurately by design, which helps to achieve "weakly connecting beam" and the desired damage control mechanism.

Stiffness changes

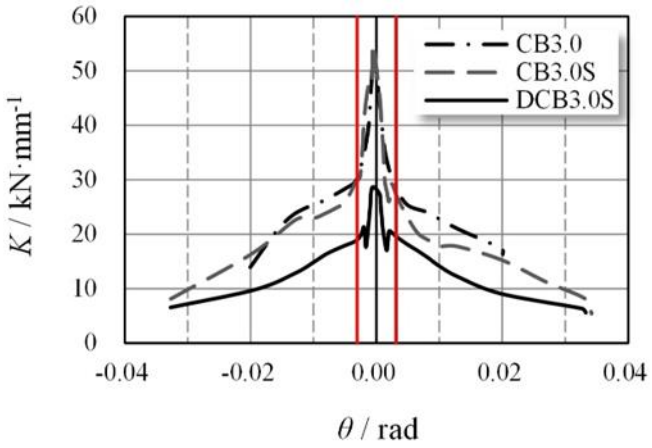

Fig.11 – Hysteretic loops and skeleton curves of specimens

Figure 11 shows the secant stiffness K of the first loading cycle of each specimen under different displacement angles. The initial stiffness of RC beam (CB3.0, CB3.0S) is about 1.9 times that of DCB3.0S with damper. The stiffness degradation trend of the three specimens was basically consistent. The position of the solid red line (θ =±1/300rad) showed a significant transition. At the end of the test ($\theta \approx \pm 1/30$rad), the stiffness of the RC beam and the beam with damper decreased to the same level.

Stiffness changes

Tab. 2- Measured strength of steel and concrete

Displacement angle θ		1/300	1/200	1/120	1/100	1/75	1/50	1/30 (1)
E_D（J×10$_3$）	CB3.0	0.19	0.81	1.24	1.22	2.92	11.22	—
	CB3.0S	0.36	0.85	1.49	1.89	4.05	11.08	16.50
	DCB3.0S	0.41	0.74	1.95	3.37	7.64	18.88	23.40
Ratio:DCB3.0S / CB3.0S		1.14	0.87	1.31	1.78	1.89	1.70	1.42

Attention:(1) θ=1/30rad Hysteretic energy dissipation at displacement Angle, ED covers the envelope area of the first force-displacement hysteretic loop, and the hysteretic energy dissipation value under the rest displacement Angle is the envelope area of two force-displacement hysteretic loops.

Table 2 shows the hysteretic energy dissipation value of each continuous beam specimen under the condition of large displacement Angle (θ greater than or equal to 1/300rad). This Table suggests that the energy dissipation level of dcb3.0s of continuous beam specimen with damper is higher than that of CB3.0 and CB3.0S of RC continuous beam specimen. To reduce the crack damage in concrete section, DCB3.0S of joint beam with damper reduces the yield and ultimate bearing capacity, while good hysteretic energy dissipation capacity can be obtained. This suggests

that the joint beam with damper exhibits better performance than RC joint beam in damage control and hysteretic energy dissipation.

To compare the deformability of the joint specimens, the yield angle θy, the peak angle θp, the limit angle θu of the test piece CB3.0S, and the yield angle θd, y of the damper in the test piece DCB3.0S are listed in Table 3. The peak angle θd, p, the limit angle θd, u, and the yield angle θc, y, the peak angle θc, p, and the limit angle θc, u of the entire beam. The Angle of the connecting beam when main longitudinal bar first yields is taken as the yield angle of the ordinary coupling beam, the angle corresponding to the peak bearing capacity is taken as the peak angle, and the angle corresponding to the bearing capacity of the skeleton line reduced to 85% of the peak bearing capacity is taken as the ultimate angle. The yield angle of the energy dissipation coupling beam takes the corresponding angles of damper and connecting beam when the strain gauge at the root of the first bending element reaches the yield strain, and the peak angle takes the corresponding Angle of damper and connecting beam when the bearing capacity reaches the peak value. The limit Angle takes the corresponding Angle at the end of the test or when the bearing capacity drops below 85% of the peak bearing capacity.

Tab. 3- Specimen deformation statistics（Unit：rad）

Damperless test piece	*θy*	*θp*		*θu*		
		Negative	*Positive*	*Negative*	*Negative*	
CB3.0	*0.0075*	*-0.016*	*-0.016*	*-0.020*	*0.020*	
CB3.0S	*0.0096*	*0.0096*	*-0.020*	*-0.03*	*0.032*	
Damper test piece	*θd,y*	*θd, p*	*θd, u*	*θc, y*	*θc, p*	*θc, u*
DCB3.0	*0.007*	*0.083*	*0.094*	*0.004*	*0.032*	*0.034*

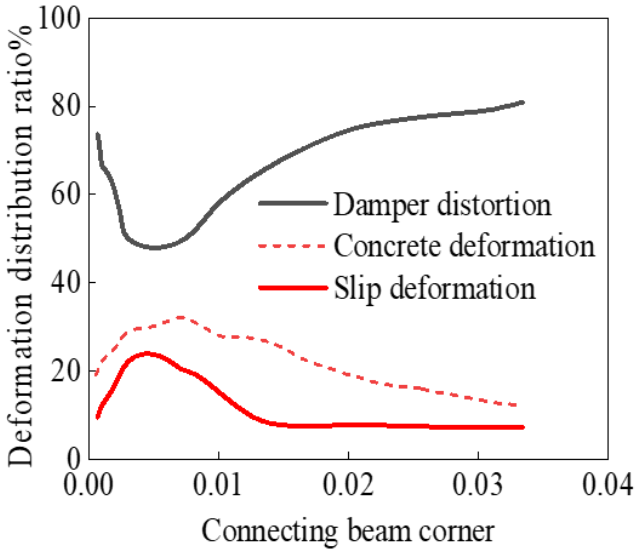

Fig.12 - Distribution of deformation of DCB3.0S specimens

It is found by comparison that the limit angles of the ordinary slab RC coupling beam and the damper coupling beam are almost the same, significantly larger than those of the ordinary slabless RC coupling beam. This reveals that the RC coupling beam with large shear span ratio has a strong ultimate deformation capability. Nevertheless, when the damper coupling beam is yielded, the damper angle and the overall angle of the coupling beam will be smaller than the yield angle of the ordinary coupling beam. Jiang Huanjun [10] et al. studied the relationship between the displacement angle of the RC shear wall structure and the deformation of the coupling beam. The results of numerous dynamic elastoplastic analysis suggest that the geometrical relationship

between the coupling beam and the adjacent wall more significantly affects the angle $K_{ij} = \theta_{ij}^{b} / \theta_i$ (θ_{ij}^{b} is the angle of the arbitrary beam of the i-th layer of the structure, θ_i is the interlayer displacement angle of the i-th layer of the structure). Based on the examples provided, it is roughly inferred that the maximum angle factor of the shear wall structure with a shear span ratio of 3.0 is about 3.0~3.5. In other words, when the displacement angle between the structural layers ranges from 1/875~1/750, the damper coupling beam will belong to the yielding state, thereby earlier consuming energy and protecting the concrete beam section.

The deformation of each part of DCB3.0S of the energy-saving coupling beam was measured, e.g. the bending and shear deformation of the concrete part at both ends of the coupling beam, and the slip of the bolt between the embedded part and the damper and the embedded part. How the deformation of the damper was distributed is shown in Figure 11. In the initial stage of loading, the deformation of damper took up low proportion since the slip deformation of the connecting bolt developed faster in the initial stage, and the proportion of the deformation of the spliced beam was relatively high. As the loading continued, the proportion of the damper deformation gradually increased, and the proportion of the concrete portion and the slip deformation was inclined to decrease. More than 80% of the total deformation at 3.3% of the beam angle was concentrated in the damper. The concrete and slip deformation ratio were nearly 10%, suggesting that the concrete part deformation is relatively small, which can effectively control the concrete damage.

CONCLUSION

Given the super-strong bearing capacity of reinforced concrete "weakly connected beam" with relatively large width and height, the energy dissipation joint beam with steel plate damper was proposed in this study. First, the yield and peak bearing capacity of the joint beam can be accurately calculated by the design equation. Second, the damage state of the joint beam can be adequately controlled. To test the seismic performance of the scheme, the performance of ordinary RC beam and damper energy dissipation beam in the quasi-static test was compared, and the following conclusions were drawn.

(1) The design equation of energy dissipation and coupling beam capacity used here can accurately calculate its yield and peak bearing capacity.

(2) To reduce the damage degree of concrete section of energy-dissipating connecting beam, the strength reduction method was used to design energy dissipating connecting beam, resulting in its stiffness lower than that of RC connecting beam, which may affect its elastic design under frequent earthquake.

(3) The damper joint beam is superior to the conventional RC joint beam in hysteretic energy dissipation, which is more obvious in the case of large deformation.

ACKNOWLEDGEMENTS

This study was supported by the National Natural Science Foundation of China (Grant No: 51108484) and Construction research project of Zhejiang provincial of China (Grant No:2013Z104).Our gratitude is also extended to reviewers for their efforts in reviewing the manuscript and their very encouraging, insightful and constructive comments.

REFERENCES

[1] WU Yuntian,LI Yingmin,ZHANG Qi,FAN Jia.Seismic design of hybrid coupled walls in United States. Journal of Building Structures, 2011,32(12):137-144.(in Chinese)

[2] WANG Yayong. Lessons learnt from building damages in the Wenchuan earthquake: seismic concept design of buildings.Journal of Building Structures,2008,29(4):20-25 . (in Chinese)

[3] MIAO Zhiwei,YE Lieping.Study on energy dissipation mechanism control in energy-based seismic design method of reinforced concrete frame-shear-wall structure. Journal of Building Structures,2014,35(1):1-9. (in Chinese)

[4] PAN Chao , WENG Dagen. Seismic analysis and design of damping controlled coupled shear wall with vertical dampers in coupling beams.Journal of Building Structures,2012,33(10):39-43. (in Chinese)

[5] JI Xiaodong , WANG Yandong , MA Qifeng , QIAN Jiar. Experimental study on seismic behavior of replaceable steel coupling beams. .Journal of Building Structures,2015,36(10):1-10. (in Chinese)

[6] Rémy D. Lequesne, Gustavo J. Parra-Montesinos, James K. Wight. Seismic Behavior and Detailing of High-Performance Fiber-Reinforced Concrete Coupling Beams and Coupled Wall Systems. Journal of Structural Engineering, 2013(139): 1362-1370.

[7] GB 50011-2010 Code for design of concrete structures.Beijing:China Architecture＆Building Press , 2010.(in Chinese)

[8] Bentz E, Collins M P. Response-2000, user manual. University of Toronto, Toronto, Ont, 2001.

[9] T. Hitaka, C. Matsui. Experimental Study on Steel Shear Wall with Slits . Journal of Structural Engineering, 2003, 129(5): 586-595.

[10] JIANG Huan-jun, HU Ling-ling, YING Yong. Research on relationship between displacement angle and deformation of reinforced concrete shear wall structure. Structural Engineer, 2011, 27(6): 26-33. (in Chinese)